



Original Article

Hepatoprotective effects and antioxidant, antityrosinase activities of phloretin and phloretin isonicotinyl hydrazone

Ai-Ren Zuo^{a,b}, Yan-Ying Yu^c, Qing-Long Shu^b, Li-Xiang Zheng^b, Xiao-Min Wang^b,
Shu-Hong Peng^b, Yan-Fei Xie^b, Shu-Wen Cao^{a,c,*}

^aState Key Laboratory of Food Science and Technology, Nanchang University, Nanchang, Jiangxi, China

^bJiangxi University of Traditional Chinese Medicine, Nanchang, Jiangxi, China

^cDepartment of Chemistry, Nanchang University, Nanchang, Jiangxi, China

Received May 14, 2013; accepted August 22, 2013

Abstract

Background: Acute liver damage is primarily induced by one of several causes, among them viral exposure, alcohol consumption, and drug and immune system issues. Agents with the ability to inhibit tyrosinase and protect against DNA damage caused by reactive oxygen species (ROS) may be therapeutically useful for the prevention or treatment of ROS-related diseases.

Methods: This investigation examined the hepatoprotective effects of phloretin and phloretin isonicotinyl hydrazone (PIH) on D-galactosamine (D-GalN)-induced acute liver damage in Kunming mice, as well as the possible mechanisms. The serum levels of alanine aminotransferase (ALT), aspartate aminotransferase (AST), γ -glutamyl transferase (γ -GT), alkaline phosphatase (ALP), and total bilirubin (TB) as well as the histopathological changes in mouse liver sections were determined. The antioxidant effects of phloretin, quercetin, and PIH on lipid peroxidation in rat liver mitochondria *in vitro*, 1,1-diphenyl-2-picrylhydrazyl (DPPH) or 2,2-azino-bis-(3-ethylbenzthiazoline-6-sulphonic acid) (ABTS) free radical scavenging activity *in vitro*, and supercoiled pBR322 plasmid DNA were confirmed. The experiment also examined the antityrosinase activity, inhibition type, and inhibition constant of phloretin and PIH.

Results: Phloretin, quercetin, or PIH significantly prevented the increase in serum ALT, AST, γ -GT, ALP, and TB in acute liver damage induced by D-GalN, and produced a marked reduction in the histopathological hepatic lesions. Phloretin, quercetin, or PIH also exhibited antioxidant effects on lipid peroxidation in rat liver mitochondria *in vitro*, DPPH or ABTS free radical scavenging activity *in vitro*, and supercoiled pBR322 plasmid DNA. Phloretin, quercetin, or PIH also exhibited good antityrosinase activity.

Conclusion: To the best of our knowledge, this was the first study of the hepatoprotective effects of phloretin and PIH on D-GalN-induced acute liver damage in Kunming mice as well as the possible mechanisms. This was also the first study of the lipid peroxidation inhibition activity of phloretin and PIH in liver mitochondria induced by the Fe²⁺/vitamin C (Vc) system *in vitro*, the protective effects on supercoiled pBR322 plasmid DNA, and the antityrosinase activity of phloretin and PIH.

Copyright © 2014 Elsevier Taiwan LLC and the Chinese Medical Association. All rights reserved.

Keywords: acute liver damage; antioxidant activity; antityrosinase activity; D-galactosamine; phloretin; phloretin isonicotinyl hydrazone

1. Introduction

Acute liver damage is mainly induced by a virus, alcohol, drugs, and immune system issues. The main treatment measures include administration of antioxidants and suitable support treatment. Aspartate aminotransferase (AST), alanine aminotransferase (ALT), γ -glutamyl transferase (γ -GT), alkaline phosphatase (ALP), and total bilirubin (TB) are the

Conflicts of interest: The authors declare that there are no conflicts of interest related to the subject matter or materials discussed in this article.

* Corresponding author. Dr. Shuwen Cao, State Key Laboratory of Food Science and Technology, Nanchang University, Nanchang 330047, Jiangxi, China.

E-mail address: yuyanying@ncu.edu.cn (S.-W. Cao).

most common diagnostic level indicators of liver damage. D-Galactosamine (D-GalN) is the interference agent of uridine diphosphate (UDP) in liver cells. UDP-D-GalN can hinder the biosynthesis of nucleic acid, glycoprotein, and glycogen. Finally, D-GalN can cause injury to and necrosis of liver cells, which is a common model used to observe the hepatoprotective effects of drugs.^{1,2}

Phloretin is a type of flavonoid that has beneficial anti-cancer and antioxidant properties, and is primarily derived from various species of apple. Phloretin isonicotinyl hydrazone (PIH) is a new compound synthesized by our team, which has more antioxidant activity than phloretin.³ Phloretin, whose molecular formula is $C_{15}H_{14}O_5$, is a di-hydrogen-chalcone flavonoid. Phloretin can fade melanin, making the skin whiten, with proven effects superior to kojic acid and arbutin. Additionally, phloretin is commonly used as a new type of whitening agent in cosmetics, and has many biological applications, including antioxidant activity.^{4–8}

This experiment examined the hepatoprotective effects of phloretin and PIH on D-GalN-induced acute liver damage in Kunming mice as well as the possible mechanisms. The serum levels of ALT, AST, γ -GT, ALP, and TB and histopathological changes in mouse liver sections were determined. The antioxidant effects of phloretin, quercetin, or PIH on lipid peroxidation in rat liver mitochondria *in vitro*, 1,1-diphenyl-2-picrylhydrazyl (DPPH) or 2,2-azino-bis-(3-ethylbenzthiazoline-6-sulphonic acid) (ABTS) free radical scavenging activity *in vitro*, and supercoiled pBR322 plasmid DNA were also determined. The experiment also examined the antityrosinase activity, inhibition type, and inhibition constant of phloretin, quercetin, or PIH.

2. Methods

2.1. Animals

Male and female Kunming mice (weighing 20–25 g), Sprague Dawley (SD) rats (weighing 200–220 g), and their food were obtained from the Experimental Animal Center of Jiangxi University of Traditional Chinese Medicine (Jiangxi, China). They were allowed free access to water and food. All the animals were housed in a room maintained at a temperature of $23 \pm 3^\circ\text{C}$ and a relative humidity of $50 \pm 10\%$, with artificial lighting from 8:00 AM to 8:00 PM for 1 week before and during the experiments. All experiments were performed in accordance with the Regulations of Experimental Animal Administration issued by the State Committee of Science and Technology of the People's Republic of China.

2.2. Chemicals and reagents

Diagnostic kits for ALT, AST, γ -GT, ALP, and TB were obtained from the Nanjing Jiancheng Bioengineering Institute (Nanjing, China). Also, a C3606 organization mitochondria separation reagent kit was purchased from Biyuntian (Shanghai, China). D-GalN, phloretin, quercetin, DPPH, thiobarbituric acid (TBA), and ABTS were purchased from the Sigma Chemical Company (St. Louis, MO, USA). PIH is a

new compound synthesized by our team, whose purity is more than 95%. Sodium dihydrogen phosphate, disodium phosphate, ferrous sulfate, potassium sulfate, and potassium persulfate ($K_2S_2O_8$) were of analytical grade and purchased from Sinopharm Chemical Reagent Co., Ltd (Shanghai, China). All other chemicals and solvents were of analytical grade and commercially available.

2.3. Synthesis and characterization of PIH

Phloretin (5.4854 g, 20 mmol) and isoniazid (2.8802 g, 21 mmol) were placed in a triple-neck flask and dissolved with 5 mL of ethanol. Subsequently, 50 mL of toluene and 0.5 g of p-toluene sulfonic acid were added and allowed to react for 48 hours. The synthesis route is shown in Fig. 1A. The liquid was separated three times using 40–70 μm silica gel column chromatography. The elution agents were composed of 20:1 ethyl acetate/methanol. Thin layer chromatography was carried out to detect PIH. The second component was collected and vacuum-dried to a constant weight.

A Hitachi L-2000 high-performance liquid chromatography (HPLC) instrument (Tokyo, Japan) and an Autima reversed-phase chromatography column (Tokyo, Japan) were used for the HPLC of PIH. The mobile phase was composed of 45% acetonitrile and 55% water. The volume of each sample was 10 μL and the wavelength used was 310 nm. The samples for the infrared (IR) spectrum were prepared via the potassium bromide method. The IR spectrum of PIH was measured within the scope of $400\text{--}4000\text{ cm}^{-1}$ using a Fourier transform infrared spectrometer (Tokyo, Japan). The hydrogen-1 nuclear magnetic resonance (NMR) and Carbon-13 NMR data and the HPLC and IR profiles of PIH were shown in the report.³ The yield efficiency of PIH was $68 \pm 5.3\%$.

2.4. D-GalN-induced hepatotoxicity model

Mice were randomly divided into seven groups of eight animals (4 males and 4 females) each. In the control group and D-GalN-intoxicated group, animals were given a single dose of distilled water [0.4 mL/20 g, intragastrically (ig)] daily. In the test groups, animals were given phloretin or quercetin or PIH (0.877 or 1.754 mmol/kg, 0.4 mL/20 g, ig) once daily. All administrations were conducted for 7 consecutive days. On the 7th day, all mice except those in the control group were simultaneously given a D-GalN/water mixture (800 mg/kg, 0.2 mL/20 g, intraperitoneally) 1 hour after the last administration, whereas the control group received only distilled water. Then, all animals were fasted for 16 hours and were subsequently tested for the following analysis. Because the molecular weights of these three compounds are different, the same unit mmol was used to determine comparative pharmacodynamics. For example, 0.877 mmol/kg or 1.754 mmol/kg phloretin means 240.3 mg/kg or 480.6 mg/kg, whereas 0.877 mmol/kg or 1.754 mmol/kg quercetin means 265 mg/kg or 530 mg/kg. Because the newly synthesized pure compound PIH was obtained with great difficulty, only 0.877 mmol/kg (344.7 mg/kg) PIH was used.

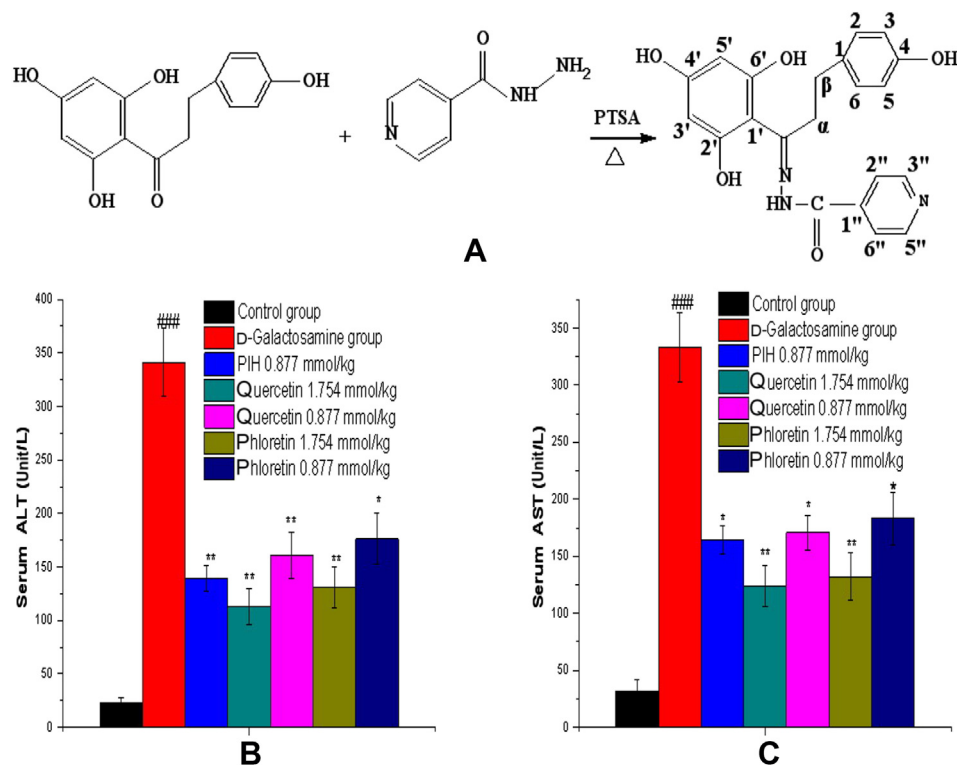


Fig. 1. (A) The synthesis of PIH. (B) The effects of phloretin, quercetin, and PIH on serum ALT activity after D-GalN treatment in mice. (C) The effects of phloretin, quercetin, and PIH on serum AST activity after D-GalN treatment in mice. ### $p < 0.001$, compared with the control group. * $p < 0.05$ and ** $p < 0.01$, compared with the D-GalN-intoxicated group. ALT = alanine aminotransferase; AST = aspartate aminotransferase; D-GalN = D-galactosamine; PIH = phloretin isonicotinyl hydrazone.

2.5. ALT, AST, γ -GT, ALP, and TB assays for monitoring liver function

Blood was taken for analysis to check ALT, AST, γ -GT, ALP, and TB levels, which were determined with commercially available diagnostic kits from Nanjing Jiancheng (Nanjing, China). Differences among the means were analyzed by one-way analysis of variance (ANOVA), and $p < 0.05$ was considered statistically significant (SPSS version 13.0; SPSS Inc., Chicago, IL, USA).

2.6. Histopathological examinations

A portion of the left lobe of the liver was preserved in formalin solution (10%) for histopathological sections. The fixed tissues were embedded in paraffin. The tissue slices with 3–5 μ m thickness were deparaffinized, dehydrated in ethanol (50–100%), and cleared by xylene. The extent of D-GalN-induced damage was evaluated by the morphological changes in liver sections stained with hematoxylin and eosin (H&E) under an Olympus light microscope. The images were examined by the Olympus BX50 light microscope. The data were analyzed by the image analysis system MetaMorph Offline (UIC/OLYMPUS).

2.7. DPPH free radical scavenging capacity

With reference to the method of Lee et al.⁹ and Wan et al.,¹⁰ the reaction system was amended to the following steps. In the

tube, 1 mL of tested samples in turn were added in different concentrations; 0.5 mL of 0.6 mmol/L DPPH methanol solution and 3.5 mL of ethanol were added. The reaction lasted 30 minutes in room temperature, in a dark environment. The wavelength used was 517 nm, and each sample was measured in triplicate and averaged. The activity was calculated according to the following formula:

$$\text{DPPH scavenging activity (\%)} = [(A_C - A_S)/A_C] \times 100\% \quad (1)$$

where A_C is the absorbance value of the control and A_S is the absorbance value of the added test samples solution.

2.8. ABTS free radical scavenging capacity

With reference to the method of Re et al.,¹¹ with some modifications, the reaction system was amended by the following steps. ABTS was dissolved in water to make a concentration of 7 mmol/L. ABTS^+ was produced by reacting the ABTS stock solution with 2.45 mmol/L $\text{K}_2\text{S}_2\text{O}_8$ and allowing the mixture to stand in the dark at room temperature for 12–16 hours prior to use. The ABTS^+ stock solution was diluted with methanol until the absorbance at 734 nm was 0.70 ± 0.02 .

Five mL of diluted ABTS^+ was added to 0.5 mL of diluted samples for 6 minutes. The activities of the samples were evaluated by comparison with a control (containing 5 mL of

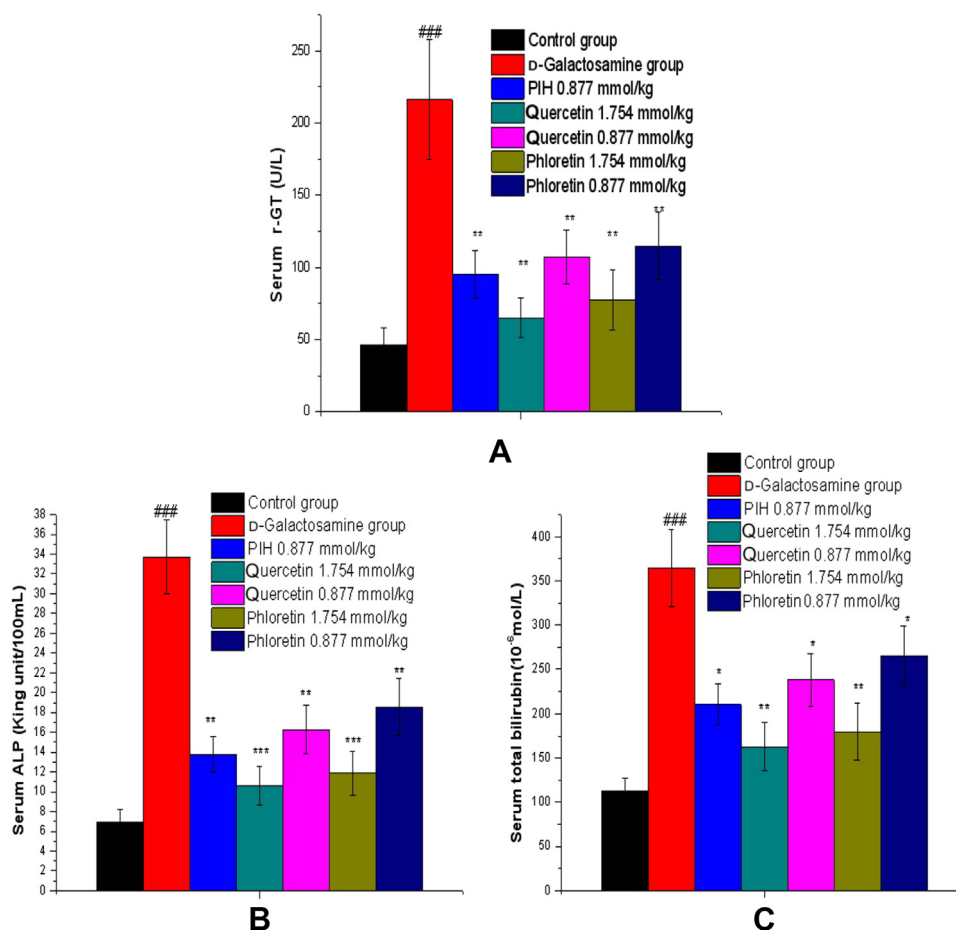


Fig. 2. (A) The effects of phloretin, quercetin, and PIH on serum γ -GT activity after D-GalN treatment in mice. (B) The effects of phloretin, quercetin, and PIH on serum ALP activity after D-GalN treatment in mice. (C) The effects of phloretin, quercetin, and PIH on serum TB activity after D-GalN treatment in mice. ### $p < 0.001$, compared with the control group. * $p < 0.05$, ** $p < 0.01$, and *** $p < 0.001$, compared with the D-GalN-intoxicated group. ALP = alkaline phosphatase; D-GalN = D-galactosamine; γ -GT = γ -glutamyl transferase; PIH = phloretin isonicotiny hydrazine; TB = total bilirubin.

ABTS⁺ solution and 0.5 mL of ethanol). Each sample was measured in triplicate and averaged. This ABTS⁺ scavenging activity was calculated by the following formula:

$$\text{ABTS}^+ \text{ scavenging activity (\%)} = [(A_C - A_S)/A_C] \times 100\% \quad (2)$$

where A_C is the absorbance value of the control and A_S is the absorbance value of the added test samples solution.

2.9. Lipid peroxidation assay in liver mitochondria *in vitro*

2.9.1. Isolation of SD rats liver mitochondria

Liver mitochondria were obtained by commercially available diagnostic kits from Biyuntian (Shanghai, China). The livers of SD rats were obtained and cut into very small pieces. Then, cold mitochondria separation reagent A was added to the liver pieces. Livers were removed and homogenized (1:2 w/v) in an ice-cold phosphate buffer (50 mM, pH 7.4) containing 0.1 mM EDTA. The homogenate was centrifuged at 40.32g for 5 minutes at 4°C. Subsequently, the supernatant was centrifuged at 13,552g for 10 minutes at 4°C. The

mitochondria pellet was resuspended in the phosphate buffer (2 g liver/mL, 1–1.3 mg protein/mL), and stored at -80°C . Prior to use, the mitochondria were thawed and washed twice with ice-cold Tris–HCl buffer (50 mM, pH 7.4) containing 150 mM KCl, followed by centrifugation at 11,000 rpm for 10 minutes at 4°C. Finally, the pellet was resuspended in 4 mL Tris–HCl buffer and then used.¹²

2.9.2. Lipid peroxidation assay

In the tubes, 0.5 mL of antioxidant solution, 1 mL of mitochondria liquid, 0.25 mL of 0.1 mM Fe²⁺, and 0.25 mL of 1 mM vitamin C were added in turn. Phosphate-buffered saline (PBS; 0.05 M, 0.5 mL) was added to the positive control group instead of the 0.5 mL of antioxidant solution. Only 1 mL of 0.05 M PBS buffer and 1 mL of mitochondrial liquid was added to the control group. The test tubes were placed at 37°C for 1 hour, then 2 mL of 20% CCl₃COOH and 2.5% hydrochloric acid solution were added for 10 minutes, followed by 2 mL of 0.67% TBA and 0.3% NaOH solution. The test tubes were placed in the water at 95°C for 30 minutes, then centrifuged at 1372g for 10 minutes. The wavelength used was 532 nm. Each sample was measured three times and averaged.

The lipid peroxidation inhibition was measured as follows:

Lipid peroxidation inhibition activity (%)

$$= [(A_C - A_S)/A_C] \times 100\% \quad (3)$$

where A_C is the absorbance value of the positive control group and A_S is the absorbance value of the added test samples solution.

2.10. Supercoiled pBR322 plasmid DNA assay

The assay was conducted following the procedure described previously with slight modification.¹³ Briefly, 100 ng of pBR322 DNA was incubated with 10 mM 2,2'-azobis(2-methylpropionamide) dihydrochloride (AAPH) in PBS (pH 7.4) to a final volume of 25 μ L (i.e., 5 μ L DNA, 15 μ L AAPH, 5 μ L antioxidants; in the absence of antioxidants, 5 μ L distilled water was used) in microcentrifuge tubes for 1 hour at 37°C. After incubation, the samples were mixed with 2 μ L 10 \times loading buffer, immediately loaded into a 0.8% agarose gel stained with 0.8 μ L gold view, and electrophoresed in a horizontal slab gel apparatus in 1 \times tris-acetate-ethylenediaminetetraacetic acid (TAE) gel buffer for 75 minutes (50 V, 20 mA). The gels were then photographed under UV transillumination using the Gel Doc XR system (Bio-Rad) (New York, America). DNA strand breaks were evaluated using the untreated DNA under the same incubation conditions as the controls. Quantity One software (Bio-Rad) was used to quantify the amount of supercoiled DNA.

2.11. Tyrosinase activity assay

Tyrosinase activity assay was performed as previously described with some modification.¹⁴ The tyrosinase activity was measured using L-3,4-dihydroxyphenylalanine (L-DOPA) as a substrate. Inhibitor samples were dissolved in dimethyl sulfoxide (DMSO) at the concentrations needed, and L-DOPA was dissolved in PBS buffer (pH 6.8) at 30°C. Then, 2.8 mL of L-DOPA (5 mM) was mixed with 0.1 mL of sample. After 1 minute, 0.1 mL of the aqueous solution of tyrosinase (5.33 μ g/mL) was added to the mixture and the absorbance was immediately monitored at 475 nm for 400 seconds. The slope of the linear part was regarded as relative enzyme activity. The inhibitory concentration 50 (IC₅₀) values, which represent the effective concentration at which 50% of enzyme activity was inhibited, were calculated to evaluate the antityrosinase activity of the different compounds. Quercetin was used as a positive control. All measurements were performed at least in triplicate. The inhibitory rate was calculated according to the formula:

$$\text{Inhibitory rate (\%)} = [(S_0 - S_1)/S_0] \times 100\% \quad (4)$$

where S_0 is the slope of the control (without samples) and S_1 is the slope in the presence of the samples.

2.12. Determination of the inhibition type and inhibition constant

The inhibition type was assayed by Lineweaver-Burk plot, and the inhibition constant was determined by the second plots of the apparent K_m/V_{mapp} or $1/V_{\text{mapp}}$ versus the concentration of the inhibitor.

3. Results

3.1. Effects of phloretin, quercetin, and PIH on serum ALT and AST activity

The results of the hepatoprotective effect of phloretin, quercetin, and PIH on serum ALT and AST activity are shown in Fig. 1B and C. In the D-GalN-intoxicated group, serum ALT and AST activities were 341.19 ± 31.35 units/L ($n = 8$, $p < 0.001$) and 332.91 ± 30.74 units/L ($n = 8$, $p < 0.001$), respectively, whereas these values were only 23.07 ± 4.39 units/L and 31.52 ± 10.11 units/L ($n = 8$), respectively, in the control group. These data indicated that D-GalN can severely damage the membrane of liver cells, causing a large number of ALT and AST enzymes to be released into the blood. Moreover, the elevated levels of serum ALT and AST were significantly reduced ($p < 0.05$) in the groups pretreated with phloretin, quercetin, and PIH (1.754 mmol/kg and 0.877 mmol/kg), and this reduction was dose-dependent. The activity order from the strongest to the weakest was PIH, quercetin, and phloretin at the same concentration of 0.877 mmol/kg. The group descriptions in the figures can be identified as different color columns. The statistical difference between low and high dose of treated compound is $p < 0.05$. Furthermore, the low dose showed significant improvement.

3.2. Effects of phloretin, quercetin, and PIH on serum γ -GT and ALP activity

The results of the hepatoprotective effect of phloretin, quercetin, and PIH on serum γ -GT and ALP activity are shown in Fig. 2A and B. In the D-GalN-intoxicated group, the serum γ -GT activity was 216.19 ± 41.86 units/L ($n = 8$, $p < 0.001$), whereas the value was only 60.70 ± 11.63 units/L ($n = 8$) in the control group. In the D-GalN-intoxicated group, the serum ALP activity was 33.69 ± 3.74 King units/100 mL ($n = 8$, $p < 0.001$), whereas the value was only 8.93 ± 1.32 King units/100 mL ($n = 8$) in the control group. These data indicated that D-GalN can severely damage the membrane of liver cells, also causing a large number of γ -GT and ALP enzymes to be released into the blood. Moreover, the elevated levels of serum γ -GT and ALP were significantly reduced ($p < 0.05$) in the groups pretreated with phloretin, quercetin, and PIH (1.754 mmol/kg and 0.877 mmol/kg), and this reduction was dose-dependent. The activity order from the strongest to the weakest was PIH, quercetin, and then phloretin, at the same concentration of 0.877 mmol/kg.

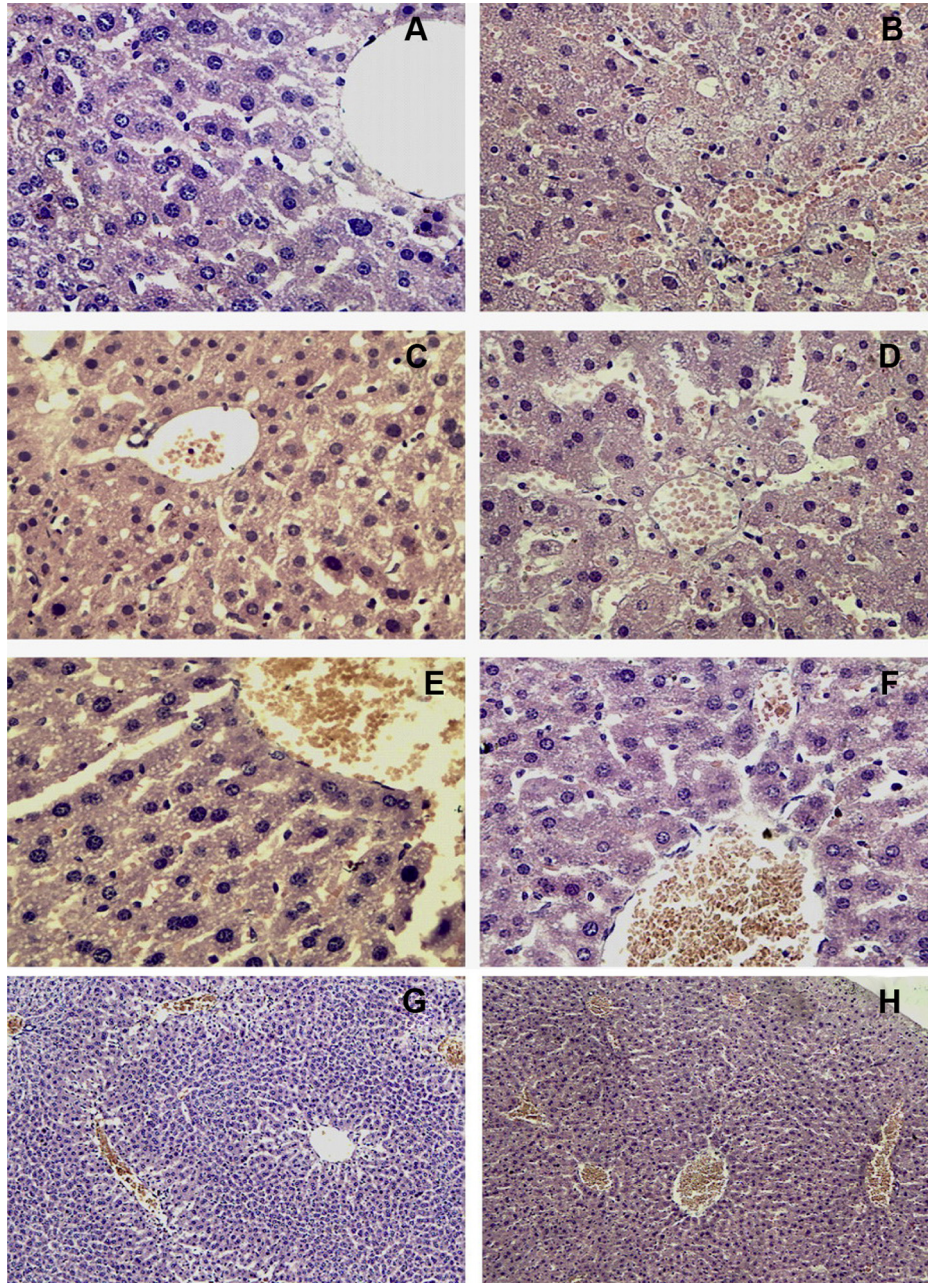


Fig. 3. The effects of phloretin, quercetin, and PIH on the liver histological damage after D-GalN treatment in mice. A portion of the left lobe of the liver tissues stained with H&E was used for histological assessment under a microscope. Representative photographs of liver sections stained with H&E showing the pathological changes in hepatic tissues under microscopy (400 \times): (A) control group; (B) D-GalN-intoxicated group; (C) quercetin 1.754 mmol/kg and D-GalN group; (D) phloretin 0.877 mmol/kg and D-GalN group; (E) PIH 0.877 mmol/kg and D-GalN group; (F) quercetin 0.877 mmol/kg and D-GalN group; (G) control group (100 \times); and (H) D-GalN-intoxicated group (100 \times). The low power fields were used to show both the portal area and central area, which are important for realizing the extent and degree of liver damage. D-GalN = D-galactosamine; H&E = hematoxylin and eosin; PIH = phloretin isonicotiny hydrazone.

3.3. Effects of phloretin, quercetin, and PIH on serum TB activity

The results of the hepatoprotective effect of phloretin, quercetin, and PIH on serum TB activity are shown in Fig. 2C. In the D-GalN-intoxicated group, the serum TB activity was $364.66 \pm 43.32 \mu\text{mol/L}$ ($n = 8$, $p < 0.001$), whereas the value was only $132.99 \pm 13.68 \mu\text{mol/L}$ ($n = 8$) in the control group. These data indicated that D-GalN can

significantly damage the membrane of liver cells, causing a large number of TB to be released into the blood. Moreover, the elevated levels of the serum TB were significantly reduced ($p < 0.05$) in the groups pretreated with phloretin, quercetin, and PIH (1.754 mmol/kg and 0.877 mmol/kg), and this reduction was dose-dependent. The activity order from the strongest to the weakest was PIH, quercetin, and then phloretin, at the same concentration of 0.877 mmol/kg.

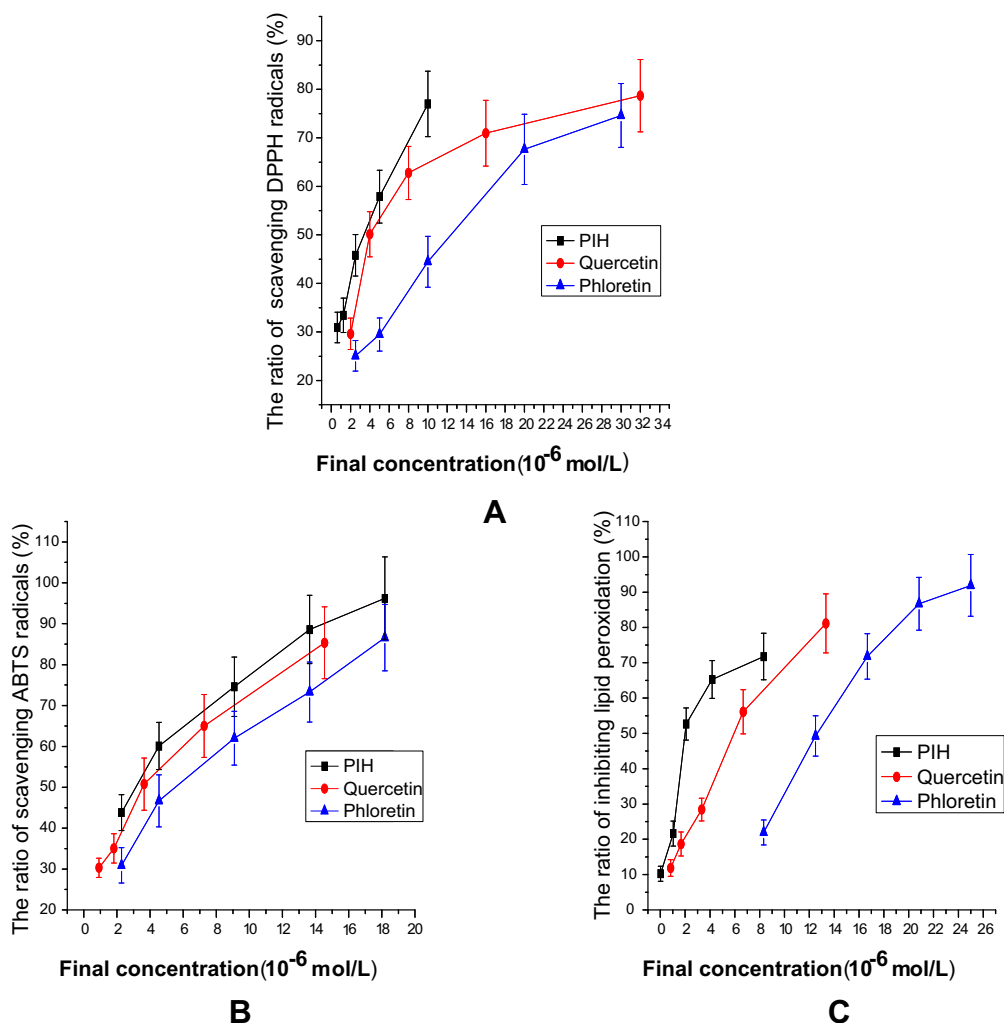


Fig. 4. (A) The relationship between final concentration and the ratio of scavenging DPPH radicals. The IC₅₀ values of scavenging DPPH free radical of PIH, quercetin, and phloretin were 2.5 $\mu\text{mol/L}$, 4 $\mu\text{mol/L}$, and 10 $\mu\text{mol/L}$, respectively ($n = 3$, $p < 0.05$). (B) The relationship between final concentration and the ratio of scavenging ABTS radicals. The IC₅₀ values of scavenging ABTS free radical of PIH, quercetin, and phloretin were 2.27 $\mu\text{mol/L}$, 3.64 $\mu\text{mol/L}$, and 4.54 $\mu\text{mol/L}$, respectively ($n = 3$, $p < 0.05$). (C) The relationship between final concentration and the ratio of inhibiting lipid peroxidation. The IC₅₀ values of inhibiting lipid peroxidation of PIH, quercetin, and phloretin were 2.08 $\mu\text{mol/L}$, 6.67 $\mu\text{mol/L}$, and 12.5 $\mu\text{mol/L}$, respectively ($n = 3$, $p < 0.01$). ABTS = 2,2-azino-bis-(3-ethylbenzthiazoline-6-sulphonic acid); DPPH = 1,1-diphenyl-2-picrylhydrazyl; IC₅₀ = inhibitory concentration 50; PIH = phloretin isonicotinyil hydrazone.

3.4. Histopathological observations

Histological assessment was used to complete the study of the hepatoprotective effects of phloretin, quercetin, and PIH on D-GalN-induced acute liver damage (Fig. 3). The histology of the liver sections of control animals showed normal hepatic cells with well-preserved cytoplasm, prominent nucleus and nucleolus, and visible central veins. The liver sections of D-GalN-intoxicated mice revealed extensive liver injuries, characterized by moderate to severe hepatocellular degeneration and necrosis around the central vein, serious gore in the liver blood sinus, inflammatory cell infiltration, ballooning degeneration, and the loss of cellular boundaries. However, the histopathological hepatic lesions were markedly ameliorated by pretreatment with phloretin, quercetin, and PIH. This was consistent with the results of serum ALT, AST, γ -GT, ALP, and TB (Figs. 1 and 2).

3.5. DPPH free radical scavenging capacity

Fig. 4A shows that PIH, quercetin, and phloretin all had significant activity in scavenging DPPH free radicals at the suitable concentration. The IC₅₀ values of scavenging DPPH free radical of PIH, quercetin, and phloretin were 2.5 $\mu\text{mol/L}$, 4 $\mu\text{mol/L}$, and 10 $\mu\text{mol/L}$ ($n = 3$), respectively. The activity order from the strongest to the weakest was PIH, quercetin, and phloretin.

3.6. ABTS free radical scavenging capacity

Fig. 4B shows that PIH, quercetin, and phloretin had significant activity in scavenging ABTS free radicals at the suitable concentration. The IC₅₀ values of scavenging ABTS free radicals of PIH, quercetin, and phloretin were 2.27 $\mu\text{mol/L}$, 3.64 $\mu\text{mol/L}$, and 4.54 $\mu\text{mol/L}$ ($n = 3$), respectively. The

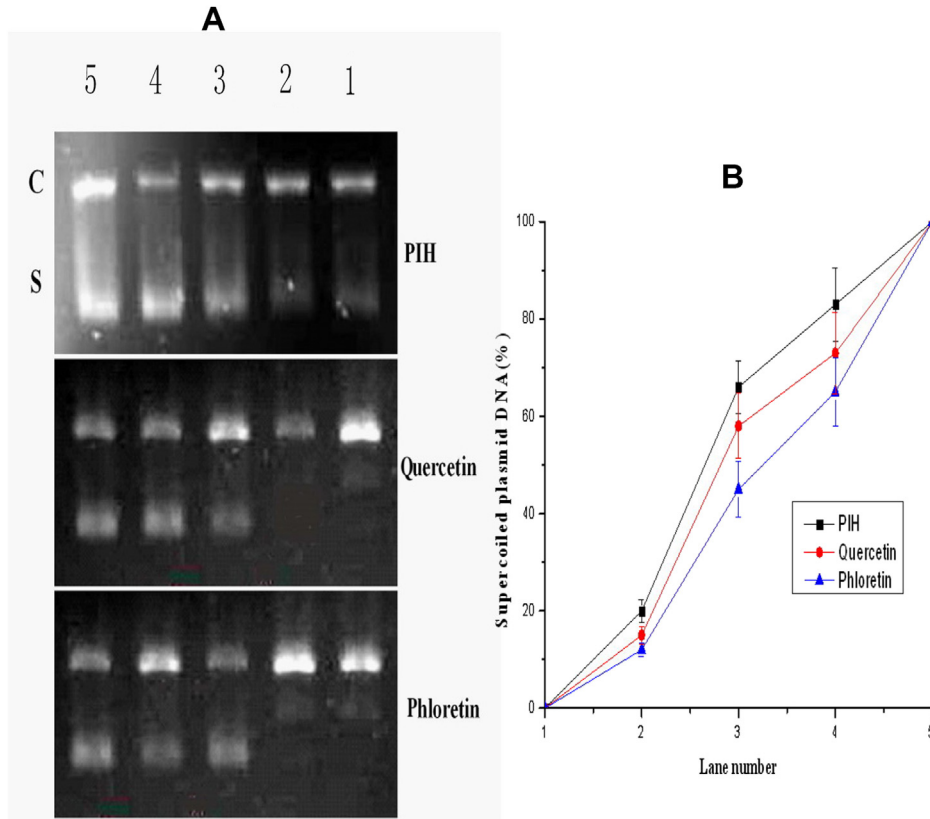


Fig. 5. (A) Agarose gel electrophoretic patterns of supercoiled pBR322 plasmid DNA converted into the open circular by AAPH in the presence or absence of samples. (B) The effects of samples on supercoiled pBR322 plasmid DNA converted into the open circular by AAPH in the presence or absence of samples. Lane 1: AAPH; lane 5: control (native pBR322 DNA, without AAPH); lanes 2–4: AAPH in the presence of samples at final concentrations of 2.5 μM , 5 μM , and 10 μM , respectively. The density of the supercoiled DNA form was quantified by Quantity One (Bio-Rad). Data are the average of three determinations. AAPH = 2,2'-azobis(2-methylpropionamide) dihydrochloride; C = open circular; S = supercoil.

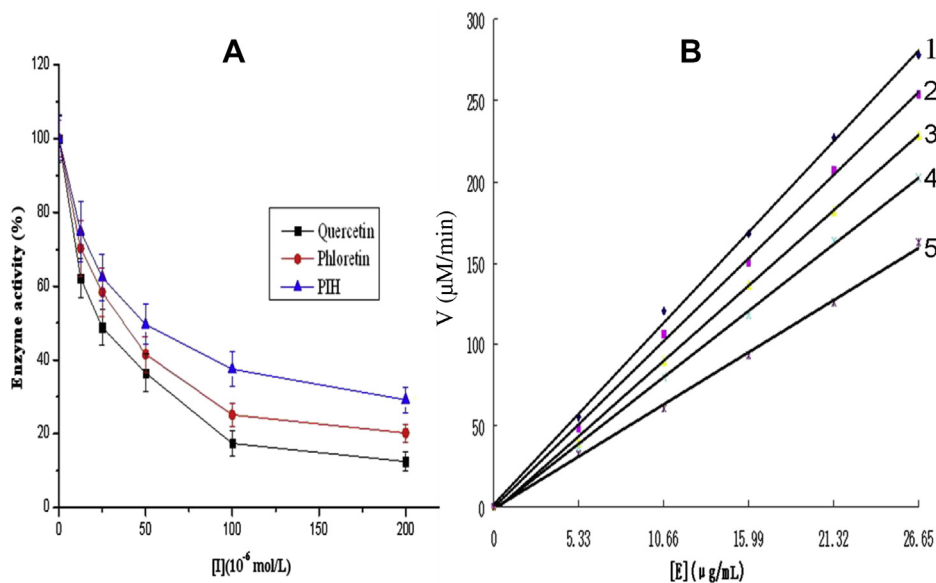


Fig. 6. (A) The inhibition effects of quercetin, phloretin, and PIH on the diphenolase activity of mushroom tyrosinase. The IC_{50} values of quercetin, phloretin, and PIH against tyrosinase were 25 μM , 37.5 μM , and 50 μM , respectively ($n = 5$, $p < 0.05$). The order of activity was: quercetin > phloretin > PIH. (B) Determination of the inhibitory mechanism of PIH on mushroom tyrosinase. The concentrations of PIH for curves 1–5 were 0 $\mu\text{mol}/\text{L}$, 12.5 $\mu\text{mol}/\text{L}$, 25 $\mu\text{mol}/\text{L}$, 50 $\mu\text{mol}/\text{L}$, and 100 $\mu\text{mol}/\text{L}$, respectively. IC_{50} = inhibitory concentration 50; PIH = phloretin isonicotinyl hydrazone.

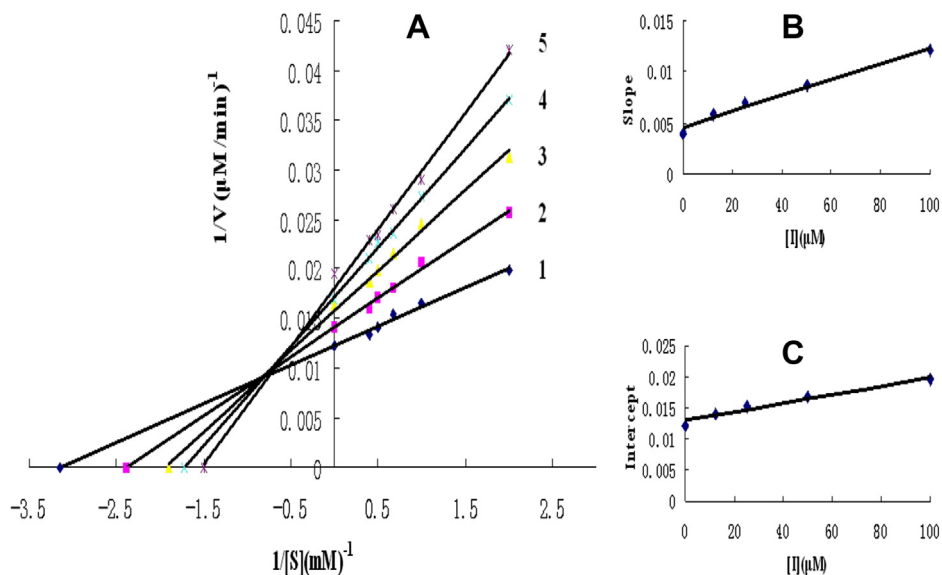


Fig. 7. Lineweaver-Burk plots for the inhibition of PIH on mushroom tyrosinase for the oxidation of L-DOPA. (A) The concentrations of PIH for curves 1–5 were 0 $\mu\text{mol/L}$, 12.5 $\mu\text{mol/L}$, 25 $\mu\text{mol/L}$, 50 $\mu\text{mol/L}$, and 100 $\mu\text{mol/L}$, respectively. (B) The plot of slope versus the concentration of PIH for determining the inhibition constants K_i . (C) The plot of intercept versus the concentration of PIH for determining the inhibition constants K_{iS} . K_i = equilibrium constant for inhibitor binding with free enzyme; K_{iS} = enzyme–substrate complex; L-DOPA = L-3,4-dihydroxyphenylalanine; PIH = phloretin isonicotinyl hydrazone.

activity order from the strongest to the weakest was PIH, quercetin, and phloretin.

3.7. Lipid peroxidation assay in liver mitochondria in vitro

Fig. 4C shows that PIH, quercetin, and phloretin had significant activity in inhibiting lipid peroxidation at suitable concentrations. The IC_{50} values of inhibiting lipid peroxidation of PIH, quercetin, and phloretin were 2.08 $\mu\text{mol/L}$, 6.67 $\mu\text{mol/L}$, and 12.5 $\mu\text{mol/L}$ ($n = 3$), respectively. The activity order from the strongest to the weakest was PIH, quercetin, and phloretin.

3.8. Supercoiled pBR322 plasmid DNA assay

As shown in Fig. 5A, the plasmid DNA was mainly supercoiled in the absence of AAPH. With the addition of 10 mM AAPH, the supercoiled form of DNA was converted into the open circular and linear forms. After the incubation of the plasmid DNA with 10 mM AAPH in the presence of the different compounds at final concentrations of 2.5 μM , 5 μM , and 10 μM , respectively, DNA damage was found to be inversely related to the concentration of the test compound. This effect was shown by a decrease in the amount of the circular and linear forms and a concomitant increase in the supercoiled form. Quantity One software (Bio-Rad) was used to quantify the amount of supercoiled DNA, and the observed values are shown in Fig. 5B. Thus, these compounds provided dose-dependent protection against AAPH-induced free radical damage. The inhibition effects produced by these compounds (10 μM) are shown in the order of activity: PIH > quercetin > phloretin.

The conversion of plasmid or bacteriophage DNA from the supercoiled form to the open circular and further linear forms

is used as an index of DNA damage.¹⁵ AAPH is water-soluble and the rate of free radical generation from AAPH can be easily controlled and measured. Thus, AAPH is extensively used as a free radical initiator for biological studies. The presence of AAPH causes strand breaks in pBR322 DNA.¹⁶

3.9. Tyrosinase activity assay

L-DOPA was used as the substrate for the diphenolase activity assay. The progress curve for the enzyme reaction was a family of lines passing through the origin with different slopes, which indicated the diphenolase activity. The results showed that the lag period did not exist as enzyme catalysis progressed in the oxidation of L-DOPA. Quercetin, phloretin, and PIH exhibited a potent inhibitory effect on diphenolase activity with dose dependence. The IC_{50} values of quercetin, phloretin, and PIH on diphenolase activity were 25 μM , 37.5 μM , and 50 μM , respectively. The activity order was quercetin > phloretin > PIH (Fig. 6A). Therefore, quercetin, phloretin, and PIH had obvious inhibitory effects on the diphenolase activity of mushroom tyrosinase.

3.10. Inhibition mechanism of phloretin and PIH on the diphenolase activity of tyrosinase

The inhibitory mechanism of phloretin and PIH on tyrosinase for oxidation of L-DOPA was studied. The inhibitors showed the same behavior. The relationship between enzyme activity and its concentration in the presence of phloretin and PIH was tested. As shown in Fig. 6B for the inhibitor of PIH, the plots of the remaining enzyme activity versus the concentration of the enzyme at different inhibitor concentrations gave a family of straight lines, which all passed through the origin. The presence of an inhibitor did not reduce the amount

of enzyme, but just resulted in the inhibition of enzyme activity. The results showed that phloretin and PIH were reversible inhibitors of tyrosinase for the oxidation of L-DOPA.

The inhibition type of phloretin and PIH was investigated by Lineweaver–Burk double-reciprocal plots. In the presence of PIH, the kinetics of the enzyme are shown in Fig. 7. The plots of $1/v$ versus $1/[S]$ gave a family of straight lines with different slopes that intercept in the second quadrant, indicating that PIH was a competitive–uncompetitive mixed type inhibitor (Fig. 7A). It can be presumed that both compounds not only can combine with free enzymes, but can also combine with enzyme–substrate complexes. The equilibrium constant for inhibitor binding with free enzyme (K_I) was obtained from a plot of the slope (K_m/V_{mapp}) versus the concentration of the inhibitor (Fig. 7B), and the enzyme–substrate complex (K_{IS}) was obtained from a plot of the vertical intercept ($1/V_{\text{mapp}}$) versus the concentration of inhibitor (Fig. 7C). The values of K_I and K_{IS} were determined as $57.5 \mu\text{M}$ and $187.1 \mu\text{M}$, respectively. Because $K_{IS} > K_I$ was in the inhibitors, the affinity of the inhibitors for the free enzyme is greater than that of the inhibitor for the enzyme–substrate complex. By contrast, phloretin was the same inhibitor type as PIH, and the inhibitor constants (K_I and K_{IS}) were estimated to be $23.5 \mu\text{M}$ and $129 \mu\text{M}$, respectively.

4. Discussion

It is well-known that the contents of serum ALT, AST, γ -GT, ALP, and TB serve as parameters to demonstrate the extent of hepatotoxicity in mice. The activities of AST and ALT are most commonly used as biochemical markers of liver damage.¹⁷ AST locates in the mitochondria whereas ALT locates in the cytoplasm. The activities of serum AST and ALT indicate the degree of cell damage (AST) or the amount of cells injured (ALT).

Liver damage induced by D-GalN is the most intensive system for xenobiotic-induced oxidative hepatotoxicity. D-GalN can induce focal necrosis of a whole hepatic lobule with severe infiltration of neutrophilic leucocytes, but liver damage can be thoroughly prevented by GdCl_3 injection in the caudal vein prior to D-GalN injection intraperitoneally in rats. Liver damage and apoptosis induced by D-GalN and a small dose of lipopolysaccharides (LPS) can be markedly alleviated via treatment with tumor necrosis factor- α (TNF- α) antiserum. Because TNF- α primarily stemmed from activated Kupffer cells (KCs), the key role that KCs played in the liver damage was thus confirmed.^{18,19}

Lipid peroxidation in liver mitochondria *in vitro* is an excellent model to study antioxidant activity. The Fe^{2+} /vitamin C (Vc) system can induce lipid peroxidation in liver mitochondria *in vitro*. Malondialdehyde (MDA) is the important product of lipid peroxidation. Thiobarbituric acid reactive substance (TBARS) is the product of MDA and TBA. TBARS can indicate the extent of lipid peroxidation. Lipid peroxidation is the oxidation degradation chain reaction of the unsaturated fatty acid. It will generate many types of free radicals,

such as oxygen free radicals, fat-oxygen free radicals, and fat-free radicals. In the terminal stage, it will generate many types of small molecules, such as MDA, which can harm cells.²⁰ Therefore, it may be beneficial to obtain adequate antioxidants in one's diet.

Phloretin can enhance adipocyte differentiation and adiponectin expression in 3T3-L1 cells,²¹ suppress the stimulated expression of endothelial adhesion molecules, and reduce the activation of human platelets.²² Phloretin can also prevent the UV-induced photodamage in human skin²³ and inhibit the oxidation of aqueous emulsions of omega-3 fatty acids and fish oil. Therefore, phloretin is a natural antioxidant in food.²⁴ Phloretin is an effective antioxidant for inhibiting the peroxidation of nitroso anions and lipids, and it also has antitumor functions. Phloretin can inhibit the proliferation of H-Ras MCF10 A human breast tumor cells in a dose-dependent manner.²⁵ It can activate c-Jun N-terminal kinase (JNK), p38 extracellular signal regulating kinase, and apoptosis protease (caspase-3), increase p53 and Bax, decrease bcl-xl, and induce apoptosis. Phloretin can also induce the apoptosis of HT-29 colon cancer cells in a dose-dependent manner. The apoptosis may be initiated by changes in the mitochondrial membrane permeability and activation of cell apoptosis protease pathways.²⁶ Additionally, phloretin can inhibit the proliferation of Molt 4 human leukemia cells *in vitro* and fisher bladder cancer cells *in vivo*. Through apoptosis experiments in melanoma B16-4 A5 cells, human leukemia cells, and HL60 cells, Kobori et al.^{27,28} found that phloretin can inhibit the movement of glucose sugar across the membrane and inhibit the activity of protein kinase C, which leads to tumor cell apoptosis. Wu et al.²⁹ found that the mRNA expression level of the type II glucose carrier in the cell membrane surface of human liver cancer cell HepG2 was five times higher than the level in normal liver cells. Phloretin can restrain the expression of the glucose carrier *in vitro* or in the body of tumor-burdened severe combined immunodeficiency (SCID) mice.

Acyl hydrazone compounds have several unique structure features as follows: (1) they contain several coordination atoms with strong coordination ability; (2) they contain coordination atoms, such as nitrogen, oxygen, and sulfur atoms, similar to the biological environment; and (3) their molecules have a greater conjugated system, with a large second harmonic generation coefficient. Acyl hydrazone compounds have several pharmacological activities, such as antibacterial, anti-inflammatory, antiviral, anti-oxidation, anticancer, and antitumor. These findings inspired the research enthusiasm of several chemists and biologists.^{30–33}

Quercetin is called a 3,3',4',5,7-five hydroxyl flavonoid, whose molecular formula is $\text{C}_{15}\text{H}_{10}\text{O}_7$. Quercetin has broad biopharmacological effects, such as antioxidant, directly scavenging free radicals, and hepatoprotectivity effects.

The study of Chen³⁴ is designed to investigate the intravenous effect of quercetin on liver damage induced by ethanol in rats. It may be deduced that quercetin, by multiple mechanism interplay, demonstrated a somewhat protective effect on liver damage induced by ethanol in rats. The study of Domitrović et al.³⁵ showed that rutin exerts stronger protection against nitrosative

stress and hepatocellular damage but has weaker antioxidant and anti-inflammatory activities and antifibrotic potential than quercetin, which may be attributed to the presence of a rutinoid moiety at position 3 of the C ring. The study of Cíntia et al.³⁶ showed that quercetin may have a preventive effect on thioacetamide-induced hepatotoxicity by modulating the oxidative stress parameters and apoptosis pathway.

Quercetin can also significantly inhibit the growth of many kinds of cancer cells such as Eca-109 cells, Lewis lung cancer, human breast cancer cells, monoblastic leukemia, BEL-7402 cells,³⁷ stomach cancer A549 cells,³⁸ colon cancer cells,³⁹ human oral squamous carcinoma cells (SCC-25),⁴⁰ and pancreatic tumor cells.⁴¹ Quercetin and isorhamnetin are the main flavonoids from *Sarcopyramis bodinieri* var. *delicate*,^{42–44} which belongs to the taxon family *Melastomataceae*, and are mainly found in Jiangxi, Fujian, and Taiwan.

The authors Zuo et al. also investigated the anticancer mechanism in HepG2 cells treated with phloretin and PIH using the 3-(4,5-dimethylthiazol-2-yl)-2,5-diphenyltetrazolium bromide (MTT) assay, flow cytometric analysis, gel electrophoresis analysis, Western blot analysis, and realtime polymerase chain reaction (PCR). The results showed that phloretin and PIH exhibited good anticancer activity at suitable concentrations. The anticancer mechanisms were as follows: inhibition of cell proliferation, blocking of cell proliferation in the G0/G1 phase of the cell cycle, degradation of the genomic DNA into a DNA ladder, reduction of the amount of human telomerase reverse transcriptase (hTERT), p53 (mutational), and Bcl-2 proteins, increase in the amount of Bax protein, and inhibition of the hTERT mRNA expression in HepG2 cells.

Tyrosinase (EC 1.14.18.1) is known to be a key enzyme for melanin biosynthesis.⁴⁵ Melanin is the pigment responsible for the color of human skin and hair; however, excessive accumulation of melanin, due to the overexpression of tyrosinase, leads to skin disorders such as age spots, freckles, melisma, and malignant melanoma.⁴⁶ In the food industry, tyrosinase is responsible for the browning of fruits and vegetables, which results in a shorter product shelf life and reduced market value.⁴⁷ By contrast, reactive oxygen species (ROS) are likely to be involved in some human physiopathologies and have been attracting growing interest from the health sector over the past few decades. Excessive amounts of ROS could induce peroxidation of membrane lipids and oxidative damage of proteins and DNA, which are generally associated with a wide variety of chronic health problems such as cancer, cardiovascular disease, and aging. Hence, agents with the ability to inhibit tyrosinase and protect against the protein and DNA damage caused by ROS may be therapeutically useful for the prevention or treatment of melanin-related and ROS related diseases. Meanwhile, applications of tyrosinase inhibitors and antioxidants as preservatives in the food industry and skin-protective ingredients in cosmetics have also drawn increased attention.

In conclusion, phloretin, quercetin, or PIH significantly prevented the increase in serum ALT, AST, γ -GT, ALP, and TB in acute liver damage induced by D-GalN, and produced a

marked amelioration in the histopathological hepatic lesions. Phloretin, quercetin, or PIH also exhibited antioxidant effects on lipid peroxidation in rat liver mitochondria *in vitro*, DPPH or ABTS free radical scavenging activity *in vitro*, and supercoiled pBR322 plasmid DNA. Phloretin, quercetin, or PIH also exhibited good antityrosinase activity.

Acknowledgments

This project was supported by the National Natural Sciences Foundation of China (No. 20962014), the Natural Sciences Foundation of Jiangxi (No. 2012ZBAB205010), the Traditional Chinese Medicine Sciences Foundation of Jiangxi (No. 2012A038), and the Sciences Foundation of Jiangxi University of Traditional Chinese Medicine (No. 2012ZR017).

References

- Li LJ, Wu ZW, Xiao DS, Sheng JF. Changes of gut flora and endotoxin in rats with D-galactosamine-induced acute liver failure. *World J Gastroenterol* 2004;**14**:2087–90.
- Nishiguchi S, Kuroki T, Takeda T, Nakajima S. Effects of putrescine on D-galactosamine-induced acute liver failure in rats. *Hepatology* 1990;**12**:348–53.
- Zuo AR, Yu YY, Li J, Cao SW. Study on the relation of structure and antioxidant activity of isorhamnetin, quercetin, phloretin, silybin and phloretin isonicotinyl hydrazone. *Free Rad Antiox* 2011;**1**:39–47.
- Rezk BM, Haenen GRMM, van der Vijgh WJF, Bast A. The antioxidant activity of phloretin: the disclosure of a new antioxidant pharmacophore in flavonoids. *Biochem Biophys Res Commun* 2002;**295**:9–13.
- Lee KW, Kim YJ, Kim DO, Lee HJ. Major phenolics in apple and their contribution to the total antioxidant capacity. *J Agric Food Chem* 2003;**51**:6516–20.
- Van Acker SABE, Van Den Berg D. Structural aspects of antioxidant activity of flavonoids. *Free Radical Bio Med* 1996;**20**:331–42.
- Miller NJ, Diplock AT. Evaluation of the total antioxidant activity as a marker of the deterioration of apple juice on storage. *J Agric Food Chem* 1995;**43**:1794–801.
- Jugd  H, Nguy D, Moller I, Cooney JM. Isolation and characterization of a novel glycosyltransferase that converts phloretin to phlorizin, a potent antioxidant in apple. *FEBS J* 2008;**75**:3804–14.
- Lee YL, Yang JH, Mau JL. Antioxidant properties of water extracts from *Monascus* fermented soybeans. *Food Chem* 2008;**106**:1127–37.
- Wan CP, Yu YY, Zhou SR, Liu W, Cao SW. Antioxidant activity and free radical-scavenging capacity of *Gynura divaricata* leaf extracts at different temperatures. *Pharmacogn Mag* 2011;**7**:40–5.
- Re R, Pellegrini N, Proteggente A. Antioxidant activity applying an improved ABTS radical cation decolorization assay. *Free Radic Biol Med* 1999;**26**:1231–7.
- Shen J, Huang C, Jiang L, Gao F. Enhancement of cisplatin induced apoptosis by suberoylanilide hydroxamic acid in human oral squamous cell carcinoma cell lines. *Biochem Pharmacol* 2007;**73**:1901–9.
- Lin X, Yang DJ, Cai WQ, Zhao QY, Gao YF, Chen Q, et al. Endomorphins, endogenous opioid peptides, provide antioxidant defense in the brain against free radical-induced damage. *Biochim Biophys Acta* 2003;**1639**:195–202.
- Chen LH, Hu YH, Song W, Song KK, Liu X, Chen QX. Synthesis and antityrosinase mechanism of benzaldehyde thiosemicarbazones: novel tyrosinase inhibitors. *J Agric Food Chem* 2012;**60**:1542.
- Ehrenfeld GM, Shipley JB, Heimbrook DC, Sugiyama H, Long EC. Copper-dependent cleavage of DNA by bleomycin. *Biochemistry* 1987;**26**:931.

16. Zhang P, Omaye S. DNA strand breakage and oxygen tension: effects of β -carotene, α -tocopherol and ascorbic acid. *Food Chem Toxicol* 2001;**39**:239.
17. Sturgill MG, Lambart GH. Xenobiotic-induced hepatotoxicity: mechanisms of liver damage and methods of monitoring hepatic function. *Clin Chem* 1997;**43**:1512–26.
18. Stachlewitz RF, Sealra V, Bradford B, Bardham CA, Rusyn I, Germolec D, et al. Glycine and uridine prevent D-galactosamine hepatotoxicity in the rat: role of kupffer cells. *Hepatology* 1999;**29**:737–45.
19. Winwood PJ, Arthur MJ. Kupffer cells: their activation and role in animal models of liver damage and human liver disease. *Semin Liver Dis* 1993;**13**:50–9.
20. Halliwell B. Vitamin C and genomic stability. *Mutat Res* 2001;**475**:29–35.
21. Hassan M, Yazidi CE, Landrier JF, Lairon D. Phloretin enhances adipocyte differentiation and adiponectin expression in 3T3-L1 cells. *Biochem Biophys Res Commun* 2007;**361**:208–13.
22. Stangl V, Lorenz M, Ludwig A. The flavonoid phloretin suppresses stimulated expression of endothelial adhesion molecules and reduces activation of human platelets. *J Nutr* 2005;**135**:172–8.
23. Oresajo C, Stephens T, Hino PD. Protective effects of a topical antioxidant mixture containing vitamin C, ferulic acid, and phloretin against ultraviolet-induced photodamage in human skin. *J Cosmetic Dermatology* 2008;**7**:290–7.
24. Vasantha Rupasinghe HP, Yasmin A. Inhibition of oxidation of aqueous emulsions of omega-3 fatty acids and fish oil by phloretin and phloridzin. *Molecules* 2010;**15**:251–7.
25. Kim MS, Kwon JY, Kang NJ. Phloretin induces apoptosis in H-ras MCF10A human breast tumor cells through the activation of p53 via JNK and p38 mitogen-activated protein kinase signaling. *Ann NY Acad Sci* 2009;**1171**:479–83.
26. Park SY, Kim EJ, Shin HK. Induction of apoptosis in HT-29 colon cancer cells by phloretin. *J Med Food* 2007;**10**:581–6.
27. Kobori M, Shinmoto H, Tsushida T. Phloretin-induced apoptosis in B16 melanoma 4A5 cells by inhibition of glucose transmembrane transport. *Cancer Lett* 1997;**119**:207–12.
28. Kobori M, Iwashita K, Shinmoto H. Phloretin-induced apoptosis in B16 melanoma 4A5 cells and HL60 human leukemia cells. *Biosci Biotechnol Biochem* 1999;**63**:719–25.
29. Wu CH, Ho YS, Tsai CY. *In vitro* and *in vivo* study of phloretin-induced apoptosis in human liver cancer cells involving inhibition of type II glucose transporter. *Int J Cancer* 2009;**124**:2210–9.
30. Hofmann J, Easmon J. New hydrazones, a novel class of experimental anti-tumor agents. *Proc Am Assoc Cancer Res* 2004;**1**:519.
31. Rodriguez-Arguelles MC, Ferrari MB. Synthesis, characterization and biological activity of Ni, Cu and Zn complexes of isatin hydrazones. *J Inorg Biochem* 2004;**98**:313–21.
32. Wang B, Yang ZY, Li T. Synthesis, characterization, and DNA-binding properties of the Ln (III) complexes with 6-hydroxy chromone-3-carbaldehyde-(2'-hydroxy) benzoyl hydrazone. *Bioorgan Med Chem* 2006;**14**:6012–21.
33. Richardson DR, Bernhardt PV. Crystal and molecular structure of 2-hydroxy-1-naphthaldehyde isonicotinoyl hydrazone (NIH) and its iron (III) complex: an iron chelator with anti-tumour activity. *J Biol Inorg Chem* 1999;**4**:266–73.
34. Chen X. Protective effects of quercetin on liver injury induced by ethanol. *Pharmacogn Mag* 2010;**6**:135–41.
35. Domitrović R, Jakovac H, Vasiljev Marchesi V, Vladimir-Knežević S, Cvijanović O, Tadić Z, et al. Differential hepatoprotective mechanisms of rutin and quercetin in CCl₄(4)-intoxicated BALB/cN mice. *Acta Pharmacol Sin* 2012;**33**:1260–70.
36. Cíntia D, Graziella R, Silvia B, Luise M. Role of quercetin in preventing thioacetamide-induced liver injury in rats. *Toxicol Pathol* 2011;**39**:949–57.
37. Teng BS, Lu YH, Wang ZT, Tao XY, Wei DZ. *In vitro* anti-tumor activity of isorhamnetin isolated from *Hippophae rhamnoides* L. against BEL-7402 cells. *Pharmacological Res* 2006;**54**:186–94.
38. Lu J, Papp LV, Fang J, Rodriguez-Nieto S, Zhivotovsky B, Holmgren A. Inhibition of mammalian thioredoxin reductase by some flavonoids: implications for myricetin and quercetin anticancer activity. *Cancer Res* 2006;**66**:4410–8.
39. Van Erk MJ, Roepman P. Integrated assessment by multiple gene expression analysis of quercetin bioactivity on anticancer-related mechanisms in colon cancer cells *in vitro*. *Eur J Nutrition* 2005;**44**:143–56.
40. Elattar TMA, Virji AS. The inhibitory effect of curcumin, genistein, quercetin and cisplatin on the growth of oral cancer cells *in vitro*. *Anticancer Res* 2000;**20**:1733–8.
41. Lee LT, Huang YT, Wang JJ. Blockade of the epidermal growth factor receptor tyrosine kinase activity by quercetin and luteolin leads to growth inhibition and apoptosis of pancreatic tumor cells. *Anticancer Res* 2002;**22**:1615–27.
42. Zuo AR, Wan CP, Zhou SR. Determination of quercetin in *Sarcopyramis bodinieri* var. *delicata* by HPLC. *Huaxiyaoxuezhazhi* 2009;**24**:300–1.
43. Zuo AR, Wang MH, Wan CP, Zhou SR. Anticancer mechanism in HepG2 cells induced by the isorhamnetin in *Sarcopyramis bodinieri* var. *delicata*. *Shizhenguoyiguoyao* 2011;**22**:427–8.
44. Wan CP, Zheng X, Chen HF. Flavonoid constituents from herbs of *Sarcopyramis bodinieri* var. *delicata*. *Chin Pharm J* 2009;**34**:172–4.
45. Han YK, Park YJ, Ha YM, Park D, Lee JY, Lee N, et al. Characterization of a novel tyrosinase inhibitor, (2R,4R)-2-(2,4-dihydroxyphenyl)thiazolidine-4-carboxylic acid (MHY384). *Biochim Biophys Acta* 2012;**1820**:542–9.
46. Fu B, Li H, Wang X, Lee FS, Cui S. Isolation and identification of flavonoids in licorice and a study of their inhibitory effects on tyrosinase. *J Agric Food Chem* 2005;**53**:7408–14.
47. Zhang JP, Chen QX, Song KK, Xie JJ. Inhibitory effects of salicylic acid family compounds on the diphenolase activity of mushroom tyrosinase. *Food Chem* 2006;**95**:579–84.